Cell Migration and Polarity on Microfabricated Gradients of Extracellular Matrix Proteins

Rico C. Gunawan,[†] Jonathan Silvestre,[†,||] H. Rex Gaskins,[‡,§] Paul J. A. Kenis,[†,§] and Deborah E. Leckband*[,†,§]

Department of Chemical and Biomolecular Engineering, Department of Animal Sciences, and Institute for Genomic Biology, University of Illinois at Urbana−Champaign, 600 South Matthews Avenue, Urbana, Illinois 61801

Received November 21, 2005. In Final Form: February 14, 2006

This paper explores the effects of the surface density and concentration profiles of extra cellular matrix proteins on the migration of rat intestinal IEC-6 cells. Microfluidic devices were used to create linear, immobilized gradients of laminin. This study investigated both the impact of the steepness and local concentrations on the directedness of cell migration. The bulk concentrations of proteins in the feed streams in the mixing device determined the gradient profile and the local concentration of laminin in the device. Two sets of gradients were used to explore cell migration directedness: (i) gradients with similar *change* in local concentration, i.e., the same gradient steepness, and (ii) different gradients with similar local concentrations. Cells migrated up the gradients, independent of the steepness of the gradients used in this study. At the same local laminin concentration, the migration rate was independent of the gradient steepness. However, cell directedness decreased significantly at high laminin densities.

Introduction

During embryonic development, cells migrate to form spatially segregated, specialized tissues. This targeted cell migration is required for proper tissue formation. For instance, the formation of the central nervous system depends on directed neurite extension and specific target identification over enormous distances.[1] In addition to morphogenesis, cell migration plays an important role in wound repair, angiogenesis, the inflammatory response, tumor cell metastasis, and tissue engineering.[2]

Numerous in vitro studies of cell migration benefited from the use of two-dimensional substrates coated with immobilized proteins and peptides.[3,4] Recent studies showed that axons turn and migrate up an adhesive peptide gradient.[5] Additionally, these substrates were used to show that migration velocity depends on the density of substratum-bound ligand, the concentration of ligand receptor, e.g., integrins, and the receptor−ligand binding affinity. These variables, in turn, affect how cells transmit the intracellular contractile force into a traction force to move forward.

In vivo, some cells migrate in response to specific patterns of such stimuli as soluble chemoattractants (chemotaxis) and surface-bound adhesion molecules (haptotaxis). In particular, substrate gradients are thought to direct cell migration in the epithelium of the small intestine[6] (Figure 1A). The intestinal epithelium consists of a monolayer of four different cell types: enterocytes, enteroendocrine cells, Paneth cells, and goblet cells.[7,8] Stem cells proliferate and undergo differentiation into one of the four cell types while migrating from the base of the crypts of Lieberkühn to the base of the villus.[9] The differentiated cells then continue to migrate upward to the tip of the villus where they are finally exfoliated into the intestinal lumen. The rate of epithelial cell migration, which was estimated from isotope tracer studies, ranged from one to two cell positions per hour.[7] The average villus residence time is thus 3−6 days.[8]

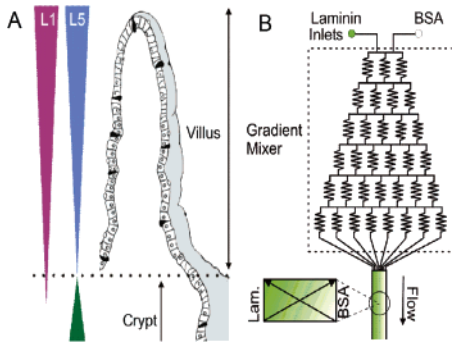

Figure 1. (A) In vivo expression profile of laminin isoforms along the crypt−villus axis of the small intestine: laminin-1 (L1), laminin-5 (L5), and laminin-2 (L2). (B) Microfluidic network design used to recreate ECM protein gradients.

Extracellular matrix (ECM) proteins beneath the epithelium reportedly influence multiple cellular functions such as proliferation, differentiation, migration, and tissue-specific gene expression.[6] Members of the integrin superfamily primarily mediate these functions. The most significant finding yet to support a possible relationship between ECM protein expression and intestinal cell functions is the spatial gradient of laminin isoforms along the crypt−villus axis (Figure 1A). The expression of laminin-1 gradually increases from the crypt−villus junction to the villus tip. Conversely, laminin-2 expression decreases with

* To whom correspondence should be addressed. Phone: 217-244-0793. Fax: 217-333-5052. E-mail: leckband@scs.uiuc.edu.
[†] Department of Chemical and Biomolecular Engineering.
[‡] Department of Animal Sciences.
[§] Institute for Genomic Biology.
[||] These authors contributed equally to this work.

(1) Helle, T.; Deiss, S.; Schwarz, U.; Schlosshauer, B. *Expt. Cell Res.* **2003**, *287*, 88−97.
(2) Lauffenburger, D. A.; Horwitz, A. F. *Cell* **1996**, *84*, 359−369.
(3) DiMilla, P.; Stone, J.; Quinn, J.; Albelda, S.; Lauffenburger, D. *J. Cell Biol.* **1993**, *122*, 729−737.
(4) Palecek, S.; Schmidt, C.; Lauffenburger, D.; Horwitz, A. *J. Cell Sci.* **1996**, *109*, 941−952.
(5) Adams, D. N.; Kao, E. Y.-C.; Hypolite, C. L.; Distefano, M. D.; Hu, W.-S.; Letourneau, P. C. *J. Neurobiol. 62*, 134−147.
(6) Beaulieu, J.-F. *Recent Work with Migration/Patterns of Expression: Cell−Matrix Interactions in Human Intestinal Cell Differentiation*.; Kluwer Academic Publishers: Hingham, MA, 1997.
(7) Potten, C.; Loeffler, M. *Development* **1990**, *110*, 1001−1020.
(8) Potten, C. S. *Philos. Trans. R. Soc. London B* **1998**, *353*, 821−830.
(9) Beaulieu, J.-F. *Front. Biosci.* **1999**, *4*, d310−321.

10.1021/la0531493 CCC: $33.50
Published on Web 04/01/2006

the distance from the base of the villus. The reciprocal expression of these laminin isoforms also complements the expression of their cell-membrane counterparts, the integrins. Hence, the relationship between the spatial patterns of laminin and integrins suggest that the migration of undifferentiated cells from the crypt may be directed to the villus by their interactions with the ECM proteins.

The effect of the surface concentration of biologically relevant molecules on cell migration (haptotaxis) has been previously demonstrated using filter-based assays.[10−12] Additionally, Varani et al.[13] used a modified Boyden chamber to create fibronectin and laminin gradients across a polycarbonate filter between two chambers. The extent of cell migration along the gradients was determined by counting the number of cells that passed through the filter. The selective cell migration to the side with the higher adsorbed protein density was indicative of laminin and fibronectin-directed haptotaxis. This approach, however, is susceptible to protein desorption from the filter.[14] Another method incorporated covalently immobilized peptides containing an adhesive RGD sequence in a polyalcrylamide gel.[15] Brandley et al.[16] showed that B16F10 melanoma cells markedly redistributed on the gel surface. The cell densities were higher at gel positions with higher peptide densities. Although these experiments indirectly showed haptotaxis, the preferential adhesion in regions of higher ligand density could also be due to the cell detachment from less-adhesive regions after rinsing the gels prior to counting. These latter methods do not allow for direct observation of individual cell migration. Additionally, the gradients prepared by these methods were not well controlled or quantified.

Recent technologies that produce better-controlled, quantifiable protein gradients include conventional lithography, electrochemical methods,[17] and soft lithography.[18−21] We recently reported the preparation of chemisorbed gradients of extracellular matrix proteins using microfluidic devices.[22] The resulting gradients enabled the high-throughput assessment of the impact of local ECM composition on cell cycle progression.

This report extends our previous investigations to determinations of the ability of laminin gradients to direct the migration of rat IEC-6 intestinal crypt-like cells. We independently quantified the impact of the local protein concentration and the gradient profile on the cell migration directedness. These findings further show that the directedness of cell migration correlates with the polarity and organization of the cell motility machinery.

Materials and Methods

Materials. Laminin was purchased from BD Biosciences (Bedford, MA). Primary anti-laminin and anti-vinculin antibodies were from Sigma (St. Louis, MO). Actin was stained with phalloidin conjugated with Texas red that was purchased from Molecular Probes (Eugene, OR). Bovine serum albumin (BSA), secondary antibody, anti-mouse IgG labeled with FITC, and sterile mineral oil were from Sigma (St. Louis, MO). Alkanethiols, 16-mercaptohexadecanoic acid (MHD) [purity > 98.5%], and 11-mercaptoundecan-1-ol (MUD) [purity > 98%] were purchased from Aldrich Chemical Co. (Milwaukee, WI). The linkers 1-ethyl-3-(3-dimethylaminopropyl) carbodiimide HCl (EDC) and *N*-hydroxysuccinimide (NHS) were obtained from Pierce (Rockford, IL). Borosilicate glass substrates were from Fisher Scientific (Pittsburgh, PA). An Antifade kit solution was from Molecular Probes.

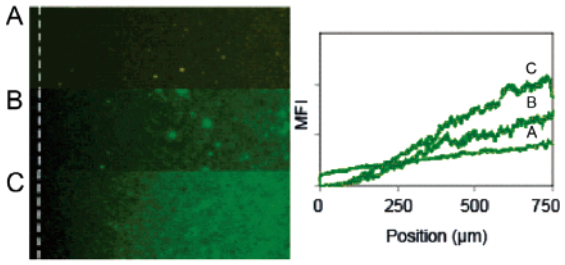

Figure 2. Fluorescence micrographs of linear gradients of laminin covalently bound to the alkanethiol monolayer. The gradient slope was adjusted by altering the initial laminin concentration: (A) 5 (10), (B) 10 (15), and (C) 25 μg/mL (34 pg/dm^2·μm).

Preparation of Uniform Protein-Coated Substrata. The ECM-coated substrates were prepared with self-assembled monolayers (SAMs) of carboxylic acid-terminated alkanethiols self-assembled on gold films that were thermally evaporated on clean glass slides. The 500-Å-thick freshly deposited gold films were thermally evaporated at a base pressure of 10^{-6} Torr onto cleaned glass slides which were precoated with a 20-Å chromium adhesion promoter. The gold films were immersed overnight in an ethanolic solution containing MHD and MUD at a 3:1 molar ratio. The coated cover slips were then rinsed with ethanol and dried under a nitrogen stream. To covalently immobilize proteins on the monolayers, the terminal carboxylic acid groups on the SAMs were activated with EDC/NHS linkers (3.8 mg EDC/mL, 6.7 mg NHS/mL in 0.5 M acetate buffer pH 5.5) for 15 min at room temperature.

To prepare uniform laminin subtrates, the activated SAMs were rinsed with the acetate buffer to remove the unreacted reagents and subsequently incubated overnight in a laminin solution at 4 °C. Laminin solutions were prepared in acetate buffer at pH 5.5 at concentrations between 5 and 50 μg/mL. The remaining reactive sites on the SAMs were then blocked by treating the cover slips for 15 min with 0.1 M glycine in phosphate-buffered saline (PBS) at pH 7.4 (10 mM phosphate, 0.14 M NaCl). Finally, the laminin-coated substrates were rinsed consecutively with PBS and sterile water and dried in air.

Preparation of Laminin Gradients. Gradients of covalently immobilized laminin were prepared in microfluidic devices as reported previously.[20−22] Microfluidic mixing tools, fabricated with poly(dimethylsiloxane) (PDMS) comprise a network of microfluidic channels (Figure 1B), with the gold substrates as the base. The freshly modified gold substrates were brought in contact with the PDMS mold and then pressed between two pieces of Plexiglass by binder clips. The microchannels were then flushed with ethanol to eliminate bubbles inside the device followed by deionized water and acetate buffer. The carboxyl groups of the MHD-containing SAMs were activated by injecting the EDC/NHS solution through the microchannels. After 15 min, the microchannels were rinsed with 0.3 mL of acetate buffer to remove the unreacted EDC/NHS reagents.

Linear laminin gradients were prepared with laminin and BSA solutions in the two injection reservoirs. BSA was used as a competing component to adjust the slope and concentration of the laminin gradients. BSA is frequently used to render biomaterial surfaces nonpermissive for cell adhesion. Across the 750-μm-wide channel, increasing laminin concentrations correspond with decreasing BSA concentrations (Figure 2). The slope of the laminin gradient could also be adjusted by altering the initial solution concentrations. The

(10) McCarthy, J.; Furcht, L. *J. Cell Biol.* **1984**, *98*, 1474−1480.
(11) McCarthy, J.; Palm, S.; Furcht, L. *J. Cell Biol.* **1983**, *97*, 772−777.
(12) McCarthy, J. B.; Basaram, M. L.; Palm, S. L.; Sas, D. F.; Furcht, L. T. *Cancer Metastasis Rev.* **1985**, *4*, 125−152.
(13) Varani, J.; Fligiel, S. E. G.; Perone, P. *Int. J. Cancer* **1985**, *35*, 559−564.
(14) Grinnell, F. *J. Cell Biol.* **1986**, *103*, 2697−2706.
(15) Brandley, B. K.; Schnaar, R. L. *Anal. Biochem.* **1988**, *172*, 270−278.
(16) Brandley, B. K. S., R. L. *Dev. Biol.* **1989**, *135*, 74−86.
(17) Plummer, S. T.; Wang, Q.; Bohn, P. W.; Stockton, R.; Schwartz, M. A. *Langmuir* **2003**, *19*, 7528−7536.
(18) Caelen, I.; Bernard, A.; Juncker, D.; Michel, B.; Heinzelmann, H.; Delamarche, E. *Langmuir* **2000**, *16*, 9125−9130.
(19) Fosser, K. A.; Nuzzo, R. G. *Anal. Chem.* **2003**, *75*, 5775−5782.
(20) Dertinger, S. K. W.; Chiu, D. T.; Jeon, N. L.; Whitesides, G. M. *Anal. Chem.* **2001**, *73*, 1240−1246.
(21) Jeon, N. L.; Dertinger, S. K. W.; Chiu, D. T.; Choi, I. S.; Stroock, A. D.; Whitesides, G. M. *Langmuir* **2000**, *16*, 8311−8316.
(22) Gunawan, R. C.; Choban, E. R.; Conour, J. E.; Silvestre, J.; Schook, L. B.; Gaskins, H. R.; Leckband, D. E.; Kenis, P. J. A. *Langmuir* **2005**, *21*, 3061−3068.

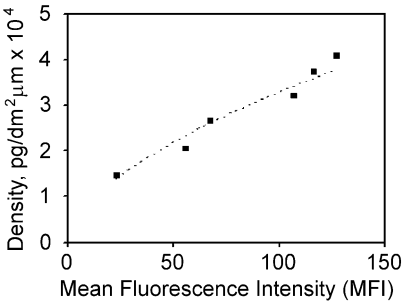

Figure 3. Laminin surface coverage versus the mean fluorescent intensity (MFI). The protein surface densities corresponding to the fluorescence readings were quantified by surface plasmon resonance.

bulk laminin concentrations used in this study ranged from 5 to 30 μg/mL, while the bulk BSA concentration was fixed at 30 μg/mL.

To covalently immobilize the gradient, a 0.2-mL solution of laminin (25, 10, and 5 μg/mL) and BSA (30 μg/mL) in 0.5 M acetate buffer at pH 5.5 were injected at a flow rate of 3.0 μL/min at 4 °C. The protein reacted with the activated SAMs to yield a covalently immobilized surface gradient. The unreacted sites on the substrate were blocked with 0.2 mL of 10% (w/w) BSA in PBS. The PDMS mold was then removed from the substrate, which was immediately treated with 10% BSA in PBS for 15 min at 4 °C to block the uncoated areas around the patterned region.

Characterization of Laminin Gradients. To visualize the laminin gradients, the patterns were stained with anti-laminin (rabbit, 1:50 in 10% BSA/PBS) for 10 min at room temperature. After the PBS rinsing, secondary antibody, anti-rabbit IgG labeled with FITC (1:200 in 10% BSA/PBS) was applied for 10 min. The substrate was then rinsed with PBS, treated with an Antifade kit to maintain the fluorescence intensity and then covered with a microscope cover slip. Fluorescent images were acquired with a Nikon Optiphot-2 epifluorescence microscope (Fryer, Carpentersville, IL) equipped with a Hammamatsu CCD camera (Hammamatsu Photonics K.K., Japan). Digital images were captured with Image-Pro Plus software, version 3.3 (Media Cybernetics, Silver Spring, MD). The fluorescence intensity was then analyzed with ImageJ software version 1.30 (NIH). Fifteen images were measured across the channel and averaged to quantify intensity variations across the gradients. The fluorescence intensity was calibrated to the protein surface coverage by comparing the mean fluorescence intensity with the protein coverage quantified by surface plasmon resonance (Figure 3).

Surface Plasmon Resonance (SPR) Measurements. The surface densities of laminin covalently bound to the SAMs were determined using an in-house-built SPR.[23] The SPR flow cell containing the SAM-modified gold substrate was initially rinsed with water and acetate buffer for 15 min. The monolayers were then activated with the EDC/NHS coupling agents for 15 min at a flow rate of 4 mL/h, followed by rinsing with acetate buffer for 5 min. Laminin was then introduced at a flow rate of 0.5 mL/h. The SPR cell was finally rinsed with acetate buffer and then water for 10 min at a flow rate of 4 mL/min. The surface density of the bound protein was determined by fitting the Fresnel reflectivity equations to the change in the plasmon resonance angle following the protein adsorption. For these analyses, we used a refractive index of 1.46 for the bound laminin.[24]

Calibration of Laminin Surface Densities. SPR was used to determine the surface densities of laminin on uniform substrates prepared with bulk laminin concentrations of 5−50 μg/mL. The mean fluorescence intensities (MFI) of laminin on the uniform substrates were obtained by immunofluorescence. The MFI was calibrated in terms of protein densities by comparing this against the amount of bound laminin determined from SPR measurements. The surface densities of the gradient were then determined using the calibration curve (Figure 3) generated from the SPR measurements and the corresponding MFIs.

(23) Lavrik, N.; Leckband, D. *Langmuir* **2000**, *16*, 1842−1851.
(24) Guemouri, L.; Ogier, L. *J. Chem. Phys.* **1998**, *109*, 3265−3268.

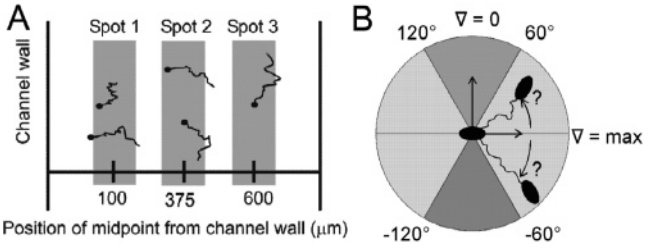

Figure 4. (A) Schematic depicting the analyzed cell migration paths on surface gradients. The width of the gradient is grouped into three 150-μm-wide regions. (B) The cell migration paths are distributed into three sectors according to the cell migration direction with respect to the steepest increase in laminin concentration.

Cell Culture. IEC-6 rat small intestine epithelial cells were cultured in Dulbecco's modified eagle medium (DMEM) supplemented with a final glucose concentration of 25 mM, 10% fetal bovine serum (FBS, Gemini Bio-Products, Woodland, CA), penicillin (10,000 U/mL), streptomycin (10 000 μg/mL, BioWhittaker, Walkersville, MD), fungizone (250 μg/mL, BioWhittaker), and 0.1 μg/mL bovine insulin (Invitrogen, Carlsbad, CA). Cells were maintained at 37 °C in a humidified incubator with a 5% CO_2 atmosphere. Cell monolayers were dissociated by incubation with trypsin−versene (BioWhittaker) for 5 min at 37 °C, resuspended in 10 mL supplemented DMEM, and centrifuged for 7 min at 1000 rpm. Cell pellets were resuspended in serum-free medium, and the cell density was determined with a hemocytometer. Cell densities of 2×10^4 cells/mL were used for cell migration assays on uniform laminin films. For determinations of the directed migration on laminin gradients, the cell density was 1×10^5 cells/mL.

Cell Migration on Uniform Laminin Substrates. A 2-mL solution containing IEC-6 cells was seeded on uniform laminin-coated gold substrates inside a 35-mm Petri dish (BD Labware, Bedford, MA). The surface of the cell medium was then covered with 2 mL of sterile mineral oil (Sigma) to minimize heat loss and water evaporation during the experiment. The Petri dish was placed on a machined metal holder used to maintain it at 37 °C by circulating water between the heating bath and the holder. The holder was fastened to the stage of an inverted Nikon Eclipse TS100 phase contrast microscope equipped with a 10× objective. A Plexiglass container was then placed over the metal holder, and the atmosphere inside the chamber was supplied with a continuous flow of 5% CO_2/95% air. The movement of cells on the laminin-coated surfaces was monitored with a Panasonic color CCD camera (Model GP-KR222), which was connected to the PixelSmart frame grabber card (High Res Technologies, Inc., Ontario, Canada). The position of each individual cell was recorded using PixelSmart data acquisition software. The cell positions were monitored every 15 min for 12 h.

Cell Migration on Laminin Gradients. After the laminin gradients were generated, the PDMS mold was removed and the uncoated regions were blocked with BSA. The thus-prepared substrate was placed inside a 60-mm Petri dish and covered with 5 mL each of cell culture medium and then mineral oil. To assess cell movement at different regions of the gradient, we recorded the migration within three spots on the 750-μm-wide gradient using time-lapse phase-contrast microscopy over a period of 6 h at 15-min time intervals. These spots, which were centered 100, 375, and 600 μm from the channel wall (starting from the low-concentration side) correspond to the low, middle, and high local concentrations of laminin within the gradient (Figure 4A). The slope of the laminin gradient was the same at each spot, as assessed by fluorescence microscopy (Figure 2). The migration paths measured within each spot were then grouped and superimposed according to the orientation of the individual migration path with respect to the direction of the steepest increase in the surface concentration of laminin (∇[laminin] = maximum). Cells that moved within a solid angle of $-60° < \theta < 60°$ relative to the maximum slope of a gradient experienced 50% of the maximum slope of ∇[laminin] of that gradient (Figure 4B). Conversely, cell migration within the direction of $60° < \theta < 120°$ and $-60° < \theta < -120°$ were considered to be random since the difference in

surface density was negligible in this direction. Cells that moved within angles of $-120° < \theta < 120°$ migrated down the gradient. We thus determined the cell migration directedness on the gradients.

Cell Migration Analysis. Images of individual cells were analyzed with the help of a cell-tracking program (CellBuster version 1.02, aXessLogic srl, Italy), which enables the manual tracking of the cell centroid position. Sixty to eighty cells were tracked on each substrate. The migration parameters, such as the cell centroid position, (x_i,y_i), and the total migration path length, were automatically recorded. The mean speed of cell migration, V_{eff}, was calculated using the methodology described by Wojciak-Stothard et al.:[25]

$$V_{\text{eff}} = \frac{S}{t} \tag{1}$$

where S is the length of the total cell migration path (mm) and t is the duration of the recording (h). The real speed of cell migration is calculated by taking into account only the time intervals when IEC-6 cells actually moved

$$V_{\text{real}} = \frac{S}{t - N} \tag{2}$$

where N is the number of time intervals when the cell did not move.

To quantify cell migration directedness relative to the gradient axis, the cell movement was observed at three spots across the gradient width (Figure 4A). The distance of the mid positions of these spots are 100, 375, and 650 μm from the channel wall where the concentration of laminin was the lowest. The cell movement was tracked within ± 75 μm from each spot. The directedness, θ, of each migration path was defined by[26,27]

$$\theta = \frac{1}{N-1} \tan^{-1}\left(\sum_{i=1}^{1=N} \frac{x_i - x_{i-1}}{y_i - y_{i-1}}\right) \tag{3}$$

where x_i and y_i are the x and y coordinates of the cell centroid at a given time and N is the number of times the cell was tracked every 15 min within 6 h ($N = 24$). The directedness was then distributed into three groups according to their relative angle with respect to the direction of the steepest laminin gradient (Figure 4B). The starting positions of each of the cell paths were superimposed so that the migration originates from a common reference point within each group.

All statistical analyses were performed using the data analysis package from MS Excel (Microsoft Corp., Seattle, WA). Means and standard deviations were calculated for cell speed. The student's *t*-test for two samples, assuming unequal variances, was used to compare the mean cell speed and the directedness between groups of results.

Immunostaining Vinculin and Actin Filaments. IEC-6 cells cultured on both uniform laminin substrates and laminin gradients were washed with PBS three times and fixed with 3.7% formaldehyde (v/v) in PBS. After 15 min, the samples were rinsed three times with PBS and blocked with 0.15 M glycine in PBS for 10 min. Cells were then permeabilized with 0.2% Triton X-100 (v/v) in PBS for 10 min and subsequently blocked with 3% (w/w) dry milk in PBS (Blotto solution) for 1 h at 4 °C, and then were incubated with 100 μL of mouse monoclonal anti-human vinculin antibody (1:100 in Blotto solution) for 1 h at 4 °C. Cells were then washed three times with PBS and incubated with 100 μL of a solution containing FITC-labeled IgG anti-mouse antibody (1:100 in Blotto solution) and phalloidin conjugated with Texas red (1:40 in Blotto solution). The samples were then washed with PBS three times and mounted on the microscope slides. An Antifade solution was applied to reduce fluorescence quenching. A coverslip was then placed on top of the fixed cells and sealed with clear nail polish. The fluorescent images of cells were viewed under a Nikon Optiphot-2 epifluorescence microscope equipped with a cooled CCD camera. Digital images were captured with Image-Pro Plus software, version 3.3.

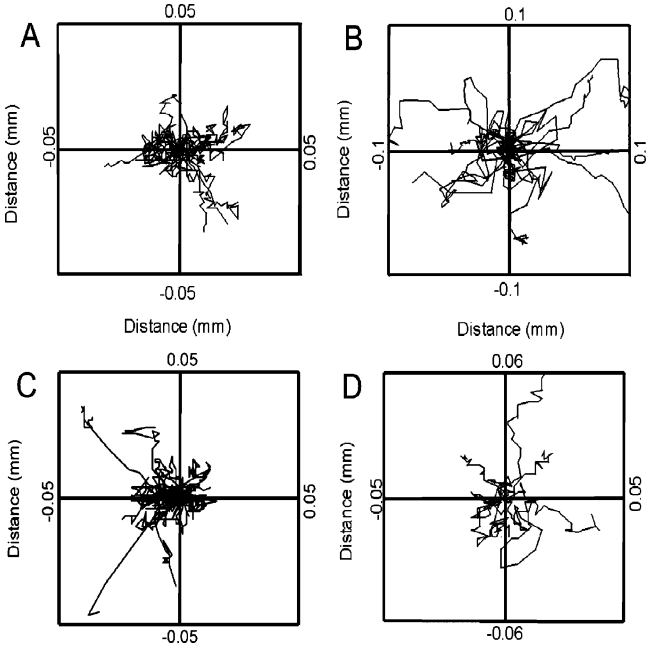

Figure 5. Migration path of IEC-6 cells on uniform laminin substrates. IEC-6 cells were cultured on laminin substrates prepared with solution concentrations of (A) 20, (B) 100, (C) 200, and (D) 500 μg/mL laminin. Continuous paths of centroid position were traced every 15 min for 12 h.

Results

1. Uniform Laminin Surface Densities.

1.1. Quantitative Analysis of Laminin Surface Coverage. The densities of the covalently bound laminin were determined from SPR measurements, which were in turn used to calibrate the laminin fluorescence intensity measurements.[22] The surface density of bound laminin was calculated from the measured change in plasmon resonance angle. The MFIs were measured with uniform laminin substrates which were obtained for each surface concentration via immunofluorescence staining. The thus-obtained relationship between the MFIs and the surface densities was used as a calibration curve for determining the local surface concentrations on the laminin gradients (Figure 3).

1.2. Cell Migration. Figure 5 shows the migration paths of individual cells on uniform laminin substrates after all the starting positions of cells on a given laminin mass coverage were superimposed to a common origin. On substrates prepared with 20 μg/mL laminin, most cells moved short distances. However, increasing the concentration of laminin 5-fold caused the cells to migrate over a 100 μm within 12 h (Figure 5B). The "wind-rose" displays of the migration paths obtained at all surface concentrations demonstrate that cells did not move preferentially in any direction, such as would occur in haptotaxis.[28] The cells moved randomly on these isotropic substrates with a migration speed that depended on the laminin surface density.

Plots of the migration speed as a function of the laminin density (Figure 6) recapitulated the bell-shaped curve reported previously.[28−30] The maximum cell migration velocity was on

(25) Wojciak-Stothard, B.; Denyer, M.; Mishra, M.; Brown, R. A. *In Vitro Cell. Dev. Biol.-Animal* **1997**, *33*, 110−117.
(26) Mardia, K. V. *Statistics of Directional Data*; Academic Press: London, 1972.
(27) Zicha, D.; Dunn, G. A.; Segal, A. W. *British J. Haemotol.* **1997**, *96*, 543−550.
(28) DiMilla, P. A.; Quinn, J. A.; Albelda, S. M.; Lauffenburger, D. A. *AIChE J.* **1992**, *38*, 1092−1104.
(29) DiMilla, P.; Barbee, K.; Lauffenburger, D. *Biophys. J.* **1991**, *60*, 15−37.
(30) Palecek, S. P.; Loftus, J. C.; Ginsberg, M. H.; Lauffenburger, D. A.; Horwitz, A. F. *Nature* **1997**, *385*, 537−540.

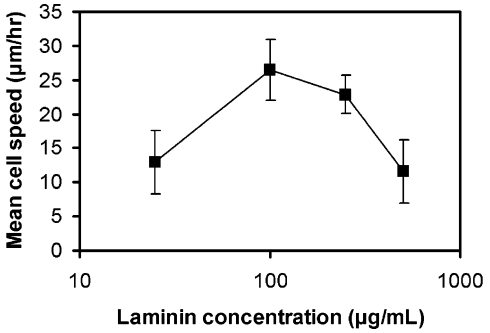

Figure 6. Mean migration speed, V_{real}, of IEC-6 cells on uniform laminin substrates. The mean cell migration speed was determined from the tracked cell positions as described in the text. The laminin concentrations are the bulk solution concentrations used to coat the substrates.

substrates generated with a laminin solution concentration of 100 μg/mL. The earlier studies indicated that a key variable governing cell migration speed is the ratio of intracellular motile force to cell-substratum attachment strength and, hence, the ligand (i.e., laminin) surface density. The data agree with the prediction that, at a given level of motile force, the migration speed should exhibit a biphasic dependence on the attachment strength (e.g., ligand density).

2. Linear Gradients of Laminin.

2.1. Laminin Surface Density Profile. The surface gradient was defined by the spatial variation in the laminin surface density across the channel. This was in turn quantified from fluorescence intensity measurements calibrated against SPR measurements. For example, in a 750-μm-wide channel, the surface density of laminin runs from 2800 to 28 200 pg/dm^2, when the bulk laminin concentration differential is 0−25 μg/mL. The slope of the gradient obtained with this feed concentration was ∇[laminin] = 34 pg/dm^2·μm (∇[laminin] $\approx$ d[laminin]/dx) (Figure 7A). Similarly, the slopes of the gradients generated with bulk laminin concentrations of 15, 10, and 5 μg/mL were 18, 15, and 10 pg/dm^2·μm, respectively. Surface gradients with a similar change in local concentration, but different local laminin densities, had a slope of 25 ± 3 pg/dm^2·μm. The bulk laminin concentration gradients used to generate these surface gradients were 5−20, 10−25, and 5−30 μg/mL (Figure 7B). These parameters are summarized in Table 1.

2.2. Cell Migration on Gradients with Similar Local Laminin Mass Coverage but Different Concentration Gradients. We anticipated that both the local concentration and local change in concentration (gradient slope) impact cell migration directedness. The microfluidic device used in this study allows

Table 1. Solution Concentrations of Laminin and Corresponding Surface Densities

laminin (μg/mL)	surface density (pg/dm^2)	gradient steepness (pg/dm^2·μm)
0−5	1950−9190	10
0−10	1690−13 000	15
0−15	2500−16 000	18
0−25	2760−28 200	34
5−20	4260−24 800	27
10−25	8650−27 900	26
5−30	14 800−31 400	22

Table 2. Directedness Probability of IEC-6 Cells on Laminin Gradients at the Local Surface Density of 7200 ± 600 pg/dm^2

solution concentration (μg/mL)	surface gradient (pg/dm^2·μm)	probability
0−5	10	63%
0−10	15	65%
0−15	18	65%
0−25	34	62%

independent control of the local concentration and the change in local concentration of the gradient. This is achieved by adjusting the solution concentration of protein used in the patterning process. Linear laminin gradients were fashioned such that the slopes differed, but the local concentration was 7200 ± 600 pg/dm^2 at a position on each gradient (Figure 7A). IEC-6 cells were seeded on these gradients, and cell directedness was quantified where the local laminin density was 7200 ± 600 pg/dm^2.

On surface gradients patterned from a solution gradient of 0−5 μg/mL, IEC-6 cells preferentially migrated toward increasing laminin concentrations, with a probability of 63%. The probability of migrating up the laminin concentration gradient was similar for surface gradients of 15, 18, and 34 pg/dm^2·μm. Thus, at the local surface concentration of 7200 ± 600 pg/dm^2, cell directedness exhibited no obvious dependence on the gradient steepness (Table 2).

The cell directedness determined at different positions on each linear gradient did depend on the local laminin surface density. For instance, at 10 pg/dm^2·μm, IEC-6 cells preferentially migrated toward increasing laminin density on all three spots, i.e., local concentrations investigated. At the local surface density of 3150 pg/dm^2, the IEC-6 cells migrated in the direction of increasing laminin with a probability of 70% (Table 2, $-60° < \theta < 60°$). However, at the local surface density of 5570 and 8000 pg/dm^2, the probability decreased to 65% and 63%, respectively. Cell migration varied similarly on the gradients prepared with a solution concentration of 0−10 and 0−15 μg/mL to give surface concentration gradients of 15 and 18 pg/dm^2·μm, respectively. On average, more than 60% of the IEC-6 cells moved toward

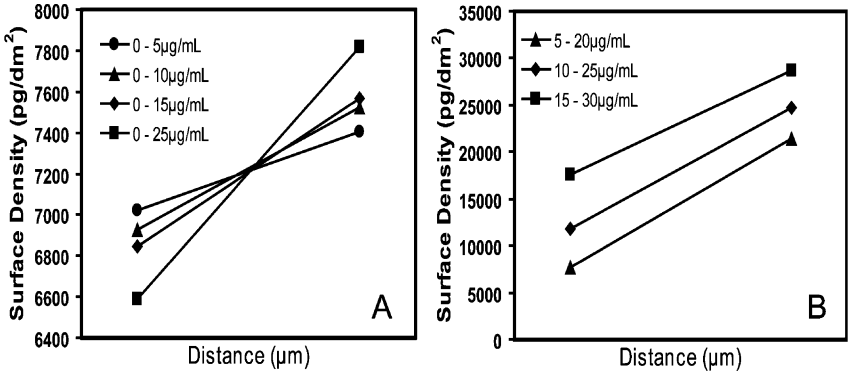

Figure 7. Gradient profiles examined: (A) Three different gradients intersect at the same local concentration of 7200 pg/dm^2. The gradients are 10 (circles), 15 (triangles), 18 (diamonds), and 34 pg/dm^2·μm (squares). (B) Three gradients with the same steepness of 25 ± 2 pg/dm^2·μm but different concentrations. The concentration ranges are in Table 1.

Table 3. Directedness Probabilities of IEC-6 Cells at Different Spatial Positions on Laminin Gradients

Θ		∇[laminin]		
		$-60° < \theta < 60°$	$\pm 60° < \theta < \pm 120°$	$-120° < \theta < 120°$
0−5 μg/mL	spot 1	70%	24%	6%
	spot 2	65%	30%	5%
	spot 3	63%	29%	8%
0−10 μg/mL	spot 1	68%	23%	9%
	spot 2	65%	24%	11%
	spot 3	63%	24%	13%
0−15 μg/mL	spot 1	66%	26%	7%
	spot 2	64%	24%	12%
	spot 3	53%	41%	6%
0−25 μg/mL	spot 1	62%	28%	10%
	spot 2	45%	36%	19%
	spot 3	35%	35%	30%
Same Gradient Steepness, Different Local Concentration				
5−20 μg/mL	spot 1	75%	25%	0%
	spot 2	61%	25%	14%
	spot 3	49%	27%	24%
10−25 μg/mL	spot 1	84%	16%	0%
	spot 2	65%	27%	8%
	spot 3	57%	29%	14%
5−30 μg/mL	spot 1	52%	28%	20%
	spot 2	50%	37%	13%
	spot 3	47%	29%	24%

increasing laminin (Table 3). However, at high laminin densities (>∼16 000 pg/dm^2), the cell directionality decreased.

On laminin gradients at 34 pg/dm^2·μm, only IEC-6 cells within spot 1 (6600 pg/dm^2) migrated in the direction of the gradient with a probability of around 60% (Table 3). The probability decreased significantly on spots 2 and 3, where the laminin density was 14250 and 21350 pg/dm^2, respectively ($p < 0.05$). A student's *t*-test verified that, at the local surface density of 21 350 pg/dm^2, the cell migration was statistically indistinguishable from a random walk ($p < 0.001$). Immunofluorescence showed that the gradient slope was constant across the entire channel (Figure 2).

2.3. Migration on Gradients with Similar Steepness but Different Local Concentration. To further investigate the effect of local laminin concentrations on cell directedness, we generated gradients with similar slopes of ∼25 ± 3 pg/dm^2·μm but different local concentrations. On linear gradients patterned from a solution concentration gradient of 5−20 μg/mL, cells migrated in the direction of the steepest slope with a probability of 74% within spot 1, i.e., 7700 pg/dm^2. On spots 2 and 3, at 14 500 and 21 400 pg/dm^2, respectively, the directedness decreased to 55% and 48%. The trend was similar for laminin gradients generated with solution gradients of 10−25 and 5−30 μg/mL (Table 3). Since these gradients all have similar slopes, the local laminin concentration clearly modulates the cell response.

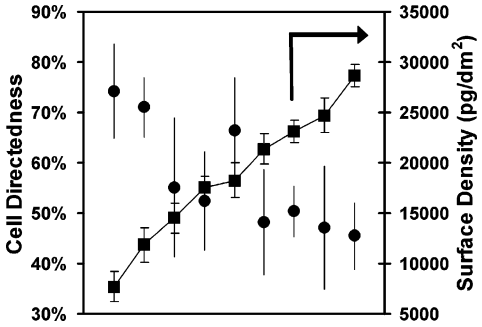

Figure 8. IEC-6 cell directednesson the same gradient but at different laminin surface densities. The filled circles indicate the cell directedness, and the filled squares show the corresponding local laminin density.

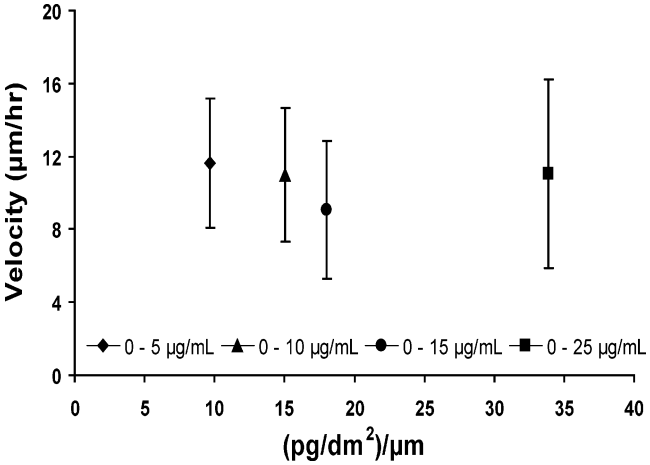

Figure 9. Cell migration velocity as a function of the gradient steepness. The mean cell migration speed was quantified on different gradients but at the same local laminin density of 7200 ± 600 pg/dm^2. At this ligand density, ∼65% of the cells migrate up the gradient (see Table 2).

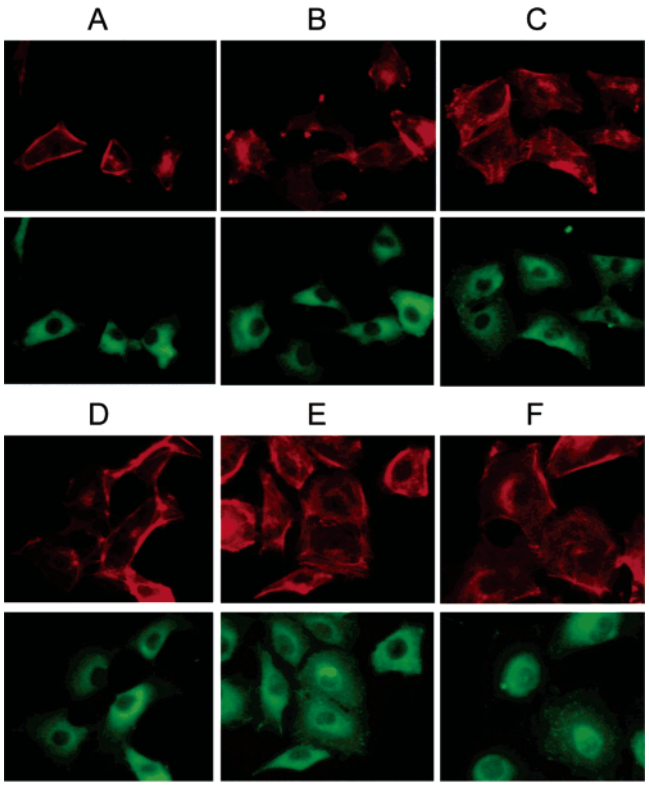

Figure 10. Morphology of IEC-6 cells on laminin substrates. Cells were cultured on uniform laminin substrates prepared with (A) 5, (B) 10, (C) 20, (D) 100, (E) 200, and (F) 500 μg/mL of laminin. After 12 h, cells were stained with antibodies directed against actin filaments (red) and vinculin (green).

Figure 8 shows the directedness of cells sensing the same spatial variation in local concentration but at different local laminin coverage. Thus, at high local concentrations, the ligand density appears to override gradient steepness in controlling the directionality of cell migration.

2.4. Dependence of Cell Migration Velocity on the Gradient Steepness. To determine whether the migration velocity depends on the gradient steepness, we quantified the mean migration velocity of cells on different gradients but at the same local laminin concentration of 7200 ± 600 pg/dm^2. At this concentration, ∼65% of the cells migrated up the gradient (Table 2, Figure

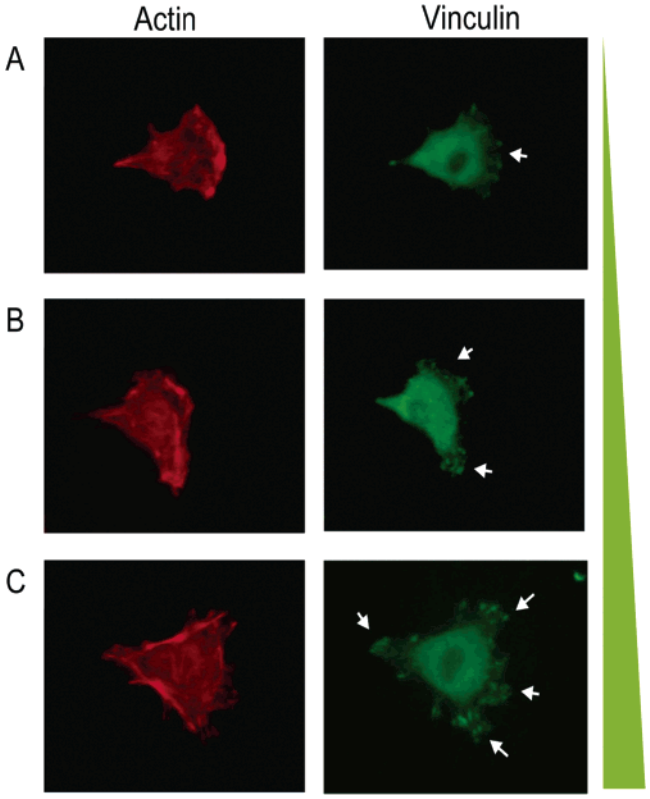

Figure 11. Morphology of IEC-6 cells on a laminin concentration gradient of 10 pg/dm^2·μm. Cells on the gradients were stained with anti-vinculin antibody (green) and phalloidin (red). The fluorescent image of cells was taken within ±75 μm of three positions on the 750-μm-wide gradients (A) 100, (B) 375, and (C) 650 μm, from the channel side where laminin concentration is the lowest. The white arrow indicates the distribution of vinculin at the front and rear ends of the cells. The green triangle indicates the surface concentration of laminin (LM).

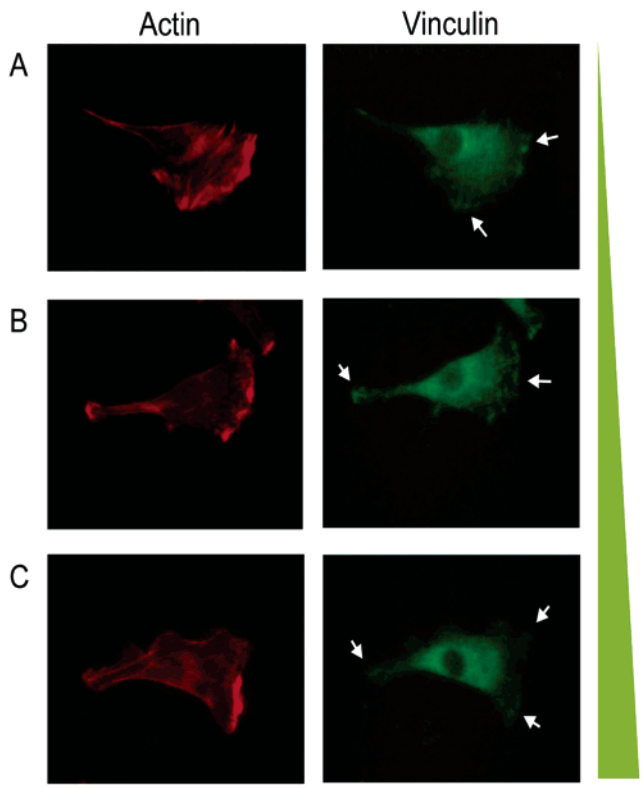

Figure 12. Morphology of IEC-6 cells on linear gradients of laminin at 15 pg/dm^2·μm. Cells on the gradients were stained with anti-vinculin antibody (green) and phalloidin (red). The fluorescent image of cells was taken within ±75 μm of three positions on the 750-μm-wide gradients (A) 100, (B) 375, and (C) 650 μm, from the channel side where laminin concentration is the lowest. The white arrow indicates the distribution of vinculin on the front and rear end of the cells. The green triangle indicates the surface concentration of laminin (LM).

8). Figure 9 summarizes the mean migration velocities measured on gradients of 10, 15, 18, and 34 pg/dm^2·μm and calculated with equation 2. Within experimental error, there was no statistically significant difference in the measured migration rates ($p > 0.05$).

3. Vinculin and Actin Localization. Migrating cells form focal adhesions at the edge of lamellipodia. One model of cell migration postulates that the adhesion sites move rearward as cells move forward over them. At the back of the cell, the adhesion sites disassemble and cells form new attachments at the cell front.[2,31] The focal adhesions also generate the traction needed for cell movement, and their distribution can affect cell migration speed and directedness. To correlate the directionality of cell migration with subcellular architecture, we imaged the focal contacts and actin filaments of IEC-6 cells on these different surfaces.

On uniform laminin films, IEC-6 cells formed multiple attachment sites around the cell periphery (Figure 10A−F). The degree of cell spreading increased with the laminin surface coverage. At low laminin densities, cells formed few attachment sites with distinct bundles of actin fibers along the cell periphery (Figure 10A−B). Vinculin was very distinct at the attachment sites but was diffuse around the nucleus. At intermediate laminin surface concentrations, cells formed additional focal contacts around the periphery and across the cell body (Figure 10C−D). Actin fibers appeared both at the cell periphery and inside the cell body, while the vinculin distribution was punctuated from the nucleus to the cell periphery. The complementary distribution of actin filaments and vinculin and the appearance of actin bundles inside the cytoplasm indicate stress fiber formation at focal adhesion sites. This is a characteristic of stable attachments.[32] The appearance of actin and vinculin was even more pronounced at higher laminin surface concentrations (Figure 10E−F).

In comparison with IEC-6 cells on uniform laminin films, IEC-6 cells on linear gradients were polarized, which is typical of slow-moving cells[2] (Figures 11−13). At the lowest laminin surface densities, actin filaments in cells on a 10 pg/dm^2·μm gradient were more concentrated at the front end than at the rear end (Figure 11A). Similarly, vinculin was punctuated around the lamellipodium and at the rear but diffuse and concentrated around the nucleus. At intermediate local surface densities, e.g., 5500 pg/dm^2, actin and vinculin were similarly distributed (Figure 11B). However, the lamellipodia broadened, and the tail end became more rounded. The extent of cell spreading and the number of focal adhesions increased in cells plated at the highest surface densities of laminin (Figure 11C). Actin filaments were distinct around the cell periphery and at both ends of cells. Additionally, vinculin was more pronounced and punctuated at the front and rear ends of cells.

On gradients of 15 pg/dm^2·μm, the trend was similar (Figure 12). However, cells appeared more elongated and spread to form larger lamellipodia. Actin filaments on all three spots appeared distinct around the cell periphery and more concentrated at the

(31) Schmidt, C.; Horwitz, A.; Lauffenburger, D.; Sheetz, M. *J. Cell Biol.* **1993**, *123*, 977−991.

(32) Friedl, P.; Brocker, E.-B. *Cell. Mol. Life Sci.* **2000**, *57*, 41−64.

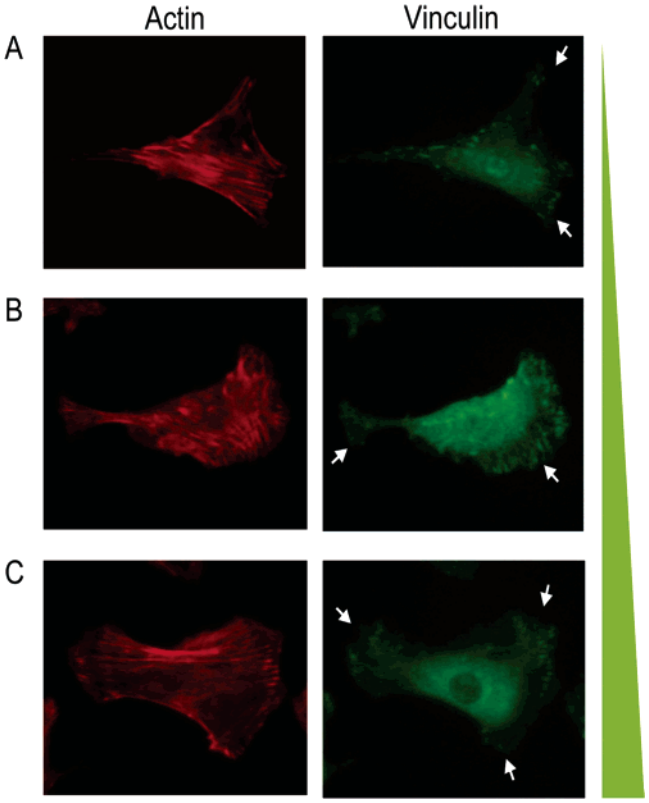

Figure 13. Morphology of IEC-6 cells on linear gradients of laminin at 34 pg/dm^2·μm. Cells on the gradients were stained with anti-vinculin antibody (green) and phalloidin (red). The fluorescent image of cells was taken within ±75 μm of three positions on the 750-μm-wide gradients (A) 100, (B) 375, and (C) 650 μm, from the channel side where laminin concentration is the lowest. The white arrow indicates the distribution of vinculin on the front and rear end of the cells. The green triangle indicates the surface concentration of laminin (LM).

front end. At the higher laminin concentrations in the gradients, vinculin appeared more punctuated at both the front and the rear end of cells, as the rear end widened (Figure 12B−C).

On gradients of 34 pg/dm^2·μm, cells formed long stress fibers (Figure 13). At the lowest local surface density, the tail ends of cells were sharp and actin formed threadlike fibers along the migration axis (Figure 13A). The distribution of vinculin was limited only to punctuated sites at the lamellipodium and at the rear end. In contrast, the rear end of cells broadened and rounded at high local laminin density (Figure 13B−C). Long stress fibers extended between the front and rear ends. The cells also form greater numbers of focal adhesions at both the front and rear of the cell, so that the difference between the front and rear is less apparent. Stress fibers also appear to be more uniform across the cells. The latter morphology correlates with reduced cell migration directedness.

Discussion

The methodology used in this study to create linear surface gradients of laminin is the same as that used previously to explore cellular processes such as chemotaxis and neurite outgrowth. Jeon et al. observed that neutrophils migrate toward increasing concentrations of chemotactic factors such as interleukin-8.[33] Similarly, Dertinger et al.[34] and Adams et al.[5] reported that neurites extend up gradients of laminin and adhesive peptides. Our results show that IEC-6 cells migrate up covalently immobilized laminin gradients prepared with a similar microfluidic gradient maker. The advantage of this technology is that it generates covalently patterned gradients with controlled mass coverage and concentration profiles. In addition, previous studies of haptotaxis relied on filtered-gel assays such as the Boyden chamber and its modifications,[15,16] but haptotaxis was inferred from the redistribution of cells at a given time period after cell plating. In contrast, these studies directly quantified both the laminin density profiles and the corresponding cell migration directedness on these profiles.

Our ability to control the laminin density profile enabled the independent investigation of the impact of local concentration and gradient steepness. In most cases, IEC-6 cells migrated toward increasing laminin on gradients of 10, 15, and 18 pg/dm^2·μm at all three positions on the gradient. However, at 34 pg/dm^2·μm, the cells migrated randomly at the intermediate and high concentration regions (Figure 13B−C).

These results show that cell migration toward increasing laminin density also depends on the local ligand concentration. To appreciate this, consider the absolute and relative changes in ligand densities over the ∼10 μm width of a cell. At 10 pg/dm^2·μm, the absolute difference in ligand density between the front and rear of a cell is 100pg/dm^2. On the steepest gradient, the difference is 340pg/dm^2. In both cases, the probability of migrating toward increasing laminin is >60% (Table 3). The cells therefore sense and respond to both of these absolute differences in ligand concentrations across the cell.

It is also possible that the dependence on ligand density is due to a lower limit of the detectable concentration differences relative to the local ligand density. For example, the concentration changes by 340 pg/dm^2 across the cell on a 34 pg/dm^2·μm gradient. This ranges from 1.2% relative to the highest laminin concentration to 12% relative to the lowest concentration on the gradient. At all but the highest density on the 5−20μg/mL gradient (Table 1), the lowest relative difference is 1%, yet cells still responded to relative density changes of ∼1% with >60% probability, except at the high laminin density.

On the basis of the data in Tables 1 and 3, the directedness drops below 60% when the local laminin concentration is >16 000 ± 2000 pg/dm^2, regardless of the gradient steepness. Increasing the gradient steepness from 10 to 34 pg/dm^2·μm at the constant ligand density of 7200 ± 600 pg/dm^2 had no observable effect on cell directedness. On the other hand, cell directedness on similar gradients of 25 ± 3 pg/dm^2·μm, but different laminin densities, decreased with increasing laminin. Thus, there appears to be threshold ligand density above which the cells are less responsive to these gradients.

A somewhat unexpected finding was the independence of the mean cell velocity on gradient steepness at similar laminin densities. The velocities are comparable to those measured on uniform substrates in the same concentration range (cf. Figure 6). This observation may be due to the modest variation in motility with ligand density and the standard deviations in the measured velocities. The migration rates only change 2-fold over the range of substrates examined (Figure 6). Much steeper gradients might therefore be needed to detect statistically significant differences in cell motility.

The correlation between cell polarization and cell directedness derives from observed differences in the numbers of focal adhesion sites and stress fibers between the front and rear of the cells. At low laminin density, the cells are more rounded due to the paucity of attachment sites and the cells cannot generate

(33) Jeon, N. L.; Baskaran, H.; Dertinger, S. K. W.; Whitesides, G. M.; VanDeWater, L.; Toner, M. *Proc. Natl. Acad. Sci. U.S.A.* **2002**, *20*, 826−830.
(34) Dertinger, S.; Jiang, X.; Li, Z.; Murthy, V. N.; Whitesides, G. M. *Proc. Natl. Acad. Sci. U.S.A.* **2002**, *99*, 12542−12547.

sufficient traction to migrate. On dense laminin substrates, the cells are well spread and do not display significant differences in the numbers of attachment sites between the front and rear of the cell. This supports the prediction that the number of focal adhesions determines the dynamics of cell movement and that asymmetry in the dynamics between the front and rear is required for directed migration.[2,4]

In conclusion, using precisely controlled surface gradients of extracellular matrix proteins, we showed that ligand concentration gradients can direct cell migration and that cell directedness depends on the local ligand concentration. Besides the laminin concentration, cell migration also depends on other variables such as the density of cell receptors (integrins)[35,36] and the integrin−ligand affinities,[37,38] which were not considered in this study. Previous investigations of the migration of epithelial cells used wound and fence assays to show the effects of uniform laminin surface densities on the migration rates of epithelial sheets.[39,40] Although those assays resembled the in vivo environments of the small intestinal epithelium, the effect of the ECM on the migration rate could not be separated from the effects of cell−cell contacts. The methodology described here permits determinations of individual migration parameters such as the migration speed and directedness as a function of the gradient steepness and the ligand concentration.

Acknowledgment. This work was supported by the University of Illinois Campus Research Initiative (D.E.L., P.J.A.K.) and by the National Science Foundation Grant No. BES 0349915 (D.E.L.).

LA0531493

(35) Bauer, J.; Schreiner, C.; Giancotti, F.; Ruoslahti, E.; Juliano, R. *J. Cell Biol.* **1992**, *116*, 477−487.
(36) Keely, P.; Fong, A.; Zutter, M.; Santoro, S. *J. Cell Sci.* **1995**, *108*, 595−607.
(37) Duband, J.; Dufour, S.; Yamada, S.; Yamada, K.; Thiery, J. *J. Cell Sci.* **1991**, *98*, 517−532.
(38) Huttenlocher, A.; Ginsberg, M.; Horwitz, A. *J. Cell Biol.* **1996**, *134*, 1551−1562.
(39) Basson, M. D.; Modlin, I. M.; Madri, J. A. *J. Clin. Invest.* **1992**, *90*, 15−23.
(40) McCormack, S. A.; Viar, M. J.; Johnson, L. R. *Am. J. Physiol. Gastrointest. Liver Physiol.* **1992**, *263*, G426−435.